SUBMITTED VERSION

Qing N. Chan, Paul R. Medwell, Bassam B. Dally, Zeyad T. Alwahabi, and Graham J. Nathan
New seeding methodology for gas concentration measurements
Applied Spectroscopy, 2012; 66(7):803-809

Published version available via DOI: http://dx.doi.org/10.1366/11-06553

New Seeding Methodology for Gas Concentration Measurements

Qing N. Chan,[1,3,*] Paul R. Medwell,[1,3] Bassam B. Dally[1,3] Zeyad T. Alwahabi,[2,3] and Graham J. Nathan[1,3]

[1]School of Mechanical Engineering, The University of Adelaide, S.A. 5005 Australia

[2]School of Chemical Engineering, The University of Adelaide, S.A. 5005 Australia

[3]Centre for Energy Technology, The University of Adelaide, S.A. 5005 Australia

*Corresponding author: shaun.chan@adelaide.edu.au

Abstract

This paper presents the first demonstration of the pulsed laser ablation technique to seed a laminar non-reacting gaseous jet at atmospheric pressure. The focused, second harmonic from a pulsed Nd:YAG laser is used to ablate a neutral indium rod at atmospheric pressure and temperature. The ablation products generated are used to seed the jet, as a marker of the scalar field. The neutral indium atoms so generated are found to be stable and survive a convection time of tens of seconds before entering the interrogation region. The measurements of laser-induced fluorescence (LIF) with indium and laser nephelometry measurements with the ablation products are both reported. The resulting average and root mean square (RMS) of the measurements are found to agree reasonably well although some differences are found. The results show that pulsed laser ablation method has potential to provide scalar measurement for for mixing studies.

1 Introduction

The mixing of two or more of gas streams is pivotal in many engineering processes, and is particularly important in fast-reacting systems, such as combustors [1]. For example, the turbulent mixing processes directly impact on the amount of soot present within a flame and on the dimensions of the soot sheets where they are found [2,3]. This is because the time-scales of soot formation and oxidation are comparable with those of mixing [4]. Likewise, the back-mixing of hot products is a technique used in certain combustors to reduce pollutant emissions and to enhance thermal efficiency [5,6]. Information regarding the mixing rates of these systems, such as concentration fluctuations, is therefore crucial to advance the understanding and the control of these processes.

Mixture fraction (ξ) is a particularly important mixing parameter, and is a conserved scalar that represents the mass fraction of reactant(s) originating form the fuel stream. This scalar is used to reduce the number of variables needed to describe the mixing processes and is used in many combustion models, such as Conditional Moment Closure (CMC) and Laminar Flamelets Model [7,8]. The measurement of mixture fraction in reacting flows is usually conducted using one or more of the key fuel components through the combination of intrusive sampling probes and gas chromatography, or through temporally and spatially resolved laser based techniques.

Many difficulties are faced in accurately measuring the mixture fraction in all parts of the flame. Both single-point and line laser-based techniques have been used for the measurement of the key species, from which the mixture fraction is deduced based on elemental conservation. Single-point measurement data, however, are unable to provide instantaneous spatial information, such as gradients, which are highly desirable for understanding turbulent flows and validating models [9]. Some two-dimensional mixture fraction imaging techniques, such as laser-induced fluorescence (LIF) of fuel, have been reported (*e.g.*, [10]). The planar imaging of the fuel is inherently difficult and has many challenges, such as the early dissociation of the fuel on the rich side of stoichiometric, optically inaccessible electronic transitions and the effect of differential diffusion [11]. Fuel tracers may be used as an alternative to the direct measurement of the fuel species. The most commonly employed tracer species for mixing studies include acetone, 3-pentanone or toluene, all of which are accessible using LIF. These tracers, however, suffer from many systematic errors that limit their applicability to the measurement of mixture fraction [11, 12]. Krypton has recently emerged as an exciting alternative [11, 12]. Being a noble gas, krypton is very stable, even in flame environments, and is therefore well suited for conserved scalar measurements [11, 12]. The LIF of krypton, however, may present some challenges as it involves a two-photon excitation process. Krypton also has the disadvantage of being expensive. Alternative tracers that have broader applicability than that the existing ones are therefore desirable.

Pulsed laser ablation is a universal tool with wide spread application, ranging from material surface processing to lithography [13–15]. The pulsed laser ablation process involves the removal of material from a surface with the use of a focused pulsed laser beam. The mechanisms associated with the ablation process are complex and are strongly dependent on the properties of the materials, as well as the parameters of the laser pulse. The laser ablation process itself is the subject of intense investigation. However, most of the current studies are motivated by the impact on the material surface being irradiated, rather than the products being generated. Nevertheless, there are also several reports on the generation of neutral atoms using laser ablation of targets such as sodium [16], aluminium [17] and indium [18]. The generation of neutral atoms is a topic of interest because of its importance in the fields such as atom optics, tokamak diagnostics, and atom lithography [16–18]. These studies, however, were typically conducted in low pressure environments. Hence insufficient information is available from the literature to assess its potential to be used to seed carrier gas at atmospheric pressure.

In light of the above gaps in knowledge, the present paper aims to investigate the potential use of the pulsed laser ablation method to generation an alternative flow tracer. Indium is chosen here as it has large oscillator strength and has electronic transition states that are optically accessible to tunable laser sources [19–21]. Indium has also been demonstrated to be a suitable thermometry species for two-line atomic fluorescence (TLAF) measurements [22, 23], so that it would be of significant practical advantage if the same seed species could be used for multiple simultaneous measurements. Hence the main aim of the paper is to examine the feasibility of using pulsed laser ablation method to generate indium atom, and to investigate the potential use of indium-LIF approach to monitor the concentration fluctuation within a jet. A secondary aim is to verify that spurious scattering from the larger ablation generated products can be effectively suppressed from the indium-LIF signal, since this is necessary for the indium-LIF approach to be used concurrently with other measurement techniques, such as particle image velocimetry (PIV). This verification is needed because, while the effective separation of indium-LIF from interference by scattering from soot has been verified [24, 25], this verification has yet to be performed for particles of micron size or larger, which are typically used for PIV seeding.

2 Methodology

The second harmonic of a Q-switched Nd:YAG laser is used to irradiate an indium rod to generate ablation products, including indium atoms, particles, and clusters. The ablation products produced using the new seeding approach are subsequently seeded into a laminar non-reacting jet. Nephelometry, using the scattered light signals from the ablation products, is employed as an alternative technique to assess the concentration fluctuation of the jet. For this feasibility study, a laminar non-reacting jet is used in the present study to avoid the complications of turbulence and the need for temperature corrections.

Indium has two optically accessible transitions, shown diagrammatically in Figure 1, which are typically used for TLAF temperature measurements [24–26]. The Stokes process involves 410.18 nm laser excitation ($5^2P_{1/2} \rightarrow 6^2S_{1/2}$ transition), and the detection of the subsequent fluorescence ($6^2S_{1/2} \rightarrow 5^2P_{3/2}$ transition) at 451.13 nm. The anti-Stokes process uses 451.13 nm excitation ($5^2P_{3/2} \rightarrow 6^2S_{1/2}$ transition) and 410.18 nm detection ($6^2S_{1/2} \rightarrow 5^2P_{1/2}$ transition). These transitions are sensitive to temperature range typically encountered in practical combustion systems (800 – 2800 K) [27].

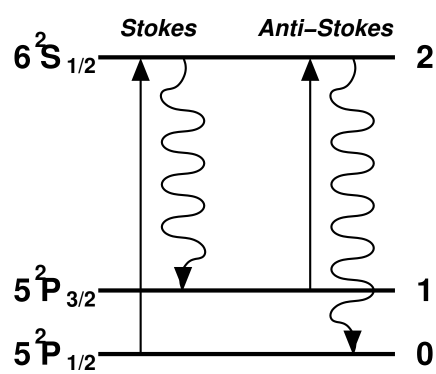

Figure 1: The indium energy transitions employed for TLAF measurements.

3 Experimental

3.1 Nozzle

The new seeding technique was assessed in a non-reacting, laminar jet in co-flow using a similar nozzle arrangement reported previously [5, 6]. The configuration consists of a central fuel jet (⌀10 mm) within an annular co-flow (⌀110 mm). The fuel jet was delivered through the nozzle into an air co-flow. The air co-flow has a fixed bulk velocity of ∼0.17 m/s and was used to improve the stability of the jet. Stainless steel mesh and a perforated plate were used to flow-condition the co-flow. A cutaway view of the nozzle arrangement used is shown in Figure 2.

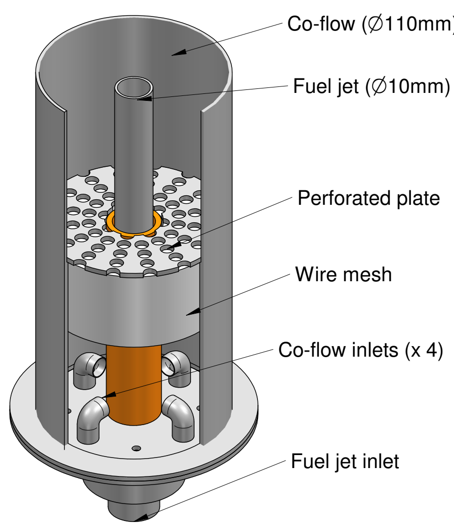

Figure 2: Cutaway view of the nozzle arrangement used to generate a jet in co-flow.

3.2 Seeder

A 10 mm diameter indium rod of 99.99% purity was placed within an 'ablation chamber' operating at atmospheric pressure. The rod was irradiated by the focused, second harmonic output (532 nm) of a Q-switched Nd:YAG laser. The resulting ablation products was transported from the chamber by the carrier gas. The indium rod was mounted on a motorized rotating shaft. This allows the indium rod to be moved in a combined rotational and translational motion to expose a 'fresh' region of the rod to each ablating shot.

Industrial grade ethylene gas ($\geq$99.5% vol. C_2H_4) was used as the carrier gas for this work. The carrier gas and the products from the ablation site were passed through a ballast volume with a motorized stirrer to damp the pulse-to-pulse variation in the generated indium, as a result of the pulsed ablation source. The addition of the ballast volume has been found to reduce the fluctuation in the signal intensity by three-fold. It is worth noting that the ablation process produces indium species, ranging from neutral, free, single atoms to particles of with a diameter of the order of milimetres. The ballast volume was therefore used here to filter out the larger particulates within the flow, as the indium-LIF signal may be susceptible to spurious scattering from such product.

3.3 Optical Arrangement

The optical arrangement consisted of three laser systems, as shown schematically in Figure 3. Two lasers were fired with ∼800 ns separation to produce the 410.18 nm and 532 nm excitation beams required for the indium-LIF and nephelometry measurements, respectively. An additional laser at 532nm was focused to ablate the indium rod.

The 410.18 nm beam required to probe the $5^2P_{1/2}\rightarrow 6^2S_{1/2}$ transition of the indium atoms was generated by a Quantel TDL 90 dye laser [22]. The 532 nm beam used for the nephelometry was generated from the second harmonic output from a Q-switched Nd:YAG laser. These beams were directed into a cylindrical telescope with a –25 mm lens followed by a +75 mm lens. The thickness of the sheets was adjusted by a plano-convex cylindrical lens with a focal length of +1000 mm. It is worth noting that these lenses are not achromatic, leading to a slight difference in their focal lengths. The effect, however, was found to be small over the measurement region. The sheets were subsequently directed through a tank, filled with fluorescing dye, in the same field of view as the nozzle. The fluorescence and scattering from the tank were used for shot-by-shot correction of the laser energy and profile variation across the sheets. The sheets were centred at ∼30 mm height above the jet exit plane. The frequency-shifted indium fluorescence signal was detected through a 10 nm bandwidth interference filter (centered at 450 nm) using another ICCD camera, with a $f_{\#}1.4$ lens. The nephelometry signal was also detected through a $f_{\#}1.4$ lens onto an intensified CCD (ICCD) camera. The gate width of the cameras was set as ∼100 ns and the timing of the cameras was set to be prompt with the corresponding laser excitation.

The output of the second harmonic (532 nm) from a high powered, Q-switched Nd:YAG laser was focused using a spherical plano-convex lens with a focal length of +200 mm into the ablation chamber. The spherical lens was affixed onto a rail system. The optimum distance between the lens and the target (*i.e.* indium rod) was determined by translating the focusing lens along the optical axis, at a fixed laser energy, until the maximum signal intensity was observed. The beam area of the ablation laser on the target used was estimated to be $\sim 7.3\times10^{-4}$ mm^2.

A centralized timing system, which consisted of a DG-535 Stanford Research Systems pulse/delay generator, was used to synchronize the lasers, the detection systems, and the computers.

4 Results and Discussion

Figure 4 presents the data obtained from a 300-shot averaged intensity of the indium Stokes fluorescence obtained in the seeded jet, as a function of the ablation laser energy. For the measurements, the LIF excitation laser fluence and the carrier gas velocity were maintained at ∼0.1 J/cm^2 and ∼0.76 m/s, respectively. These parameters were held constant to ensure that the ablation energy is the only variable. From Figure 4, it is apparent that the indium

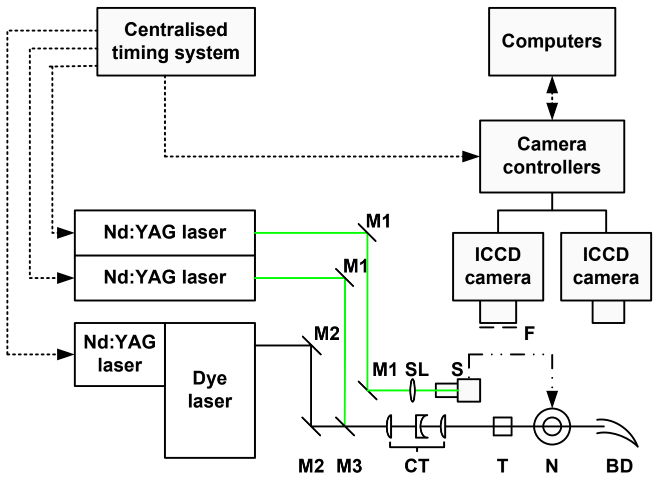

Figure 3: Schematic diagram of the experimental arrangement. BD, beam dump; CT, cylindrical telescope; F, 450 nm interference filter; S, seeder; SL, spherical lens; M1, high energy 532 nm mirror; M2, mirror; M3, dichroic mirror; N, nozzle; T, tank.

fluorescence increases with ablation energy. This is to be expected since the ablation of indium is a thermal process proceeding via the vaporisation of the metal [14]. An increase in the energy results in the vaporisation of more indium from the rod. The threshold ablation energy is $\sim 6\times 10^{-3}$ J per pulse. The threshold ablation energy is the ablation laser energy at which the indium fluorescence becomes detectable for the present arrangement. As a consequence of the investigation being conducted at atmospheric pressure, and also because of the long passage used to transport the ablation products, it is not possible to directly compare the present value with previous studies that were typically conducted at much lower pressures.

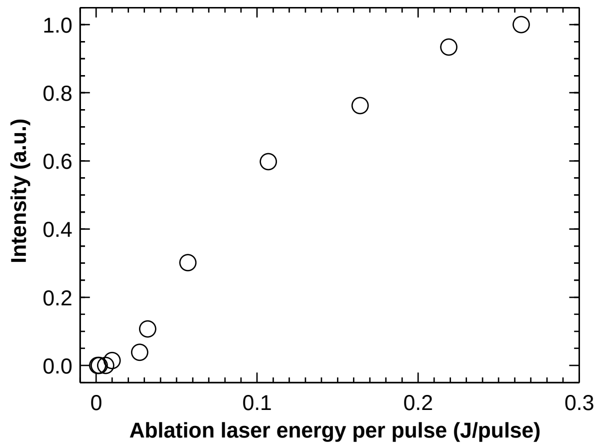

Figure 4: Measured intensity of indium fluorescence as a function of ablation laser energy per pulse.

It is also worth noting that tuning the laser off-resonance reveals that the contribution of the laser-induced interferences to the indium fluorescence signal collected at all ablation laser energies is insignificant (typically less than 1%). This observation implies that the present optical arrangement is sufficient to suppress the laser-induced interferences from the filtered ablation products. This finding also shows that the inelastic nature of the technique is insensitive to interferences from spurious scattering. This gives confidence that the indium-LIF technique is appropriate for use in other particle-laden environments, such as in the presence of particle seeding for PIV measurements.

The detection of the neutral indium atoms, despite being generated and transported from an ablation site that is remote from the nozzle, indicates that the species is not sensitive to reactions or self-collision. It is also noted the signal intensity is not significantly affected when the path length of the seeding pipe is increased. Such character of the neutral indium atoms is advantageous, as this suggests that the species may be generated at a convenient location upstream from the interrogation region.

Figures 5(a) and 5(b) present the typical single-shot fluorescence and nephelometry measurements, recorded simultaneously, for the carrier gas with a nozzle exit velocity of $\sim$1.61 m/s. For the measurements, the indium-LIF and the nephelometry excitation laser fluence were maintained at $\sim$0.1 J/cm^2 and $\sim$0.45 J/cm^2 respectively. The images presented are corrected for background, darkcharge, detector attenuation and sheet profile corrections. By appropriate image processing software, these images are also spatially matched using a four-point matching algorithm and morphed based on the cross-correlation of a target to ensure sub-pixel matching. The in-plane spatial resolution of these matched images is $\sim$0.29 mm per pixel. From the figures, it is clear that the indium LIF image is relatively more uniform in comparison with the nephelometry image, the latter of which exhibits a few spots of high intensity due to the presence of large particles or aggregations. This highlights the advantage of atomic over particle seeding in scalar measurements and also helps to explain the differences in the quantitative comparisons, discussed below.

To assess the feasibility of the technique to map the concentration profile

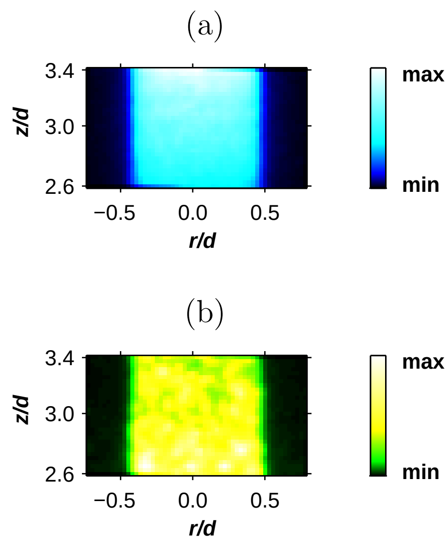

Figure 5: Typical simultaneous single-shot (a) indium-LIF, and (b) nephelometry images. Laser propagates from left to right.

of the jet, the average radial profiles $\bar{C}(r,z)$ of the indium-LIF are derived from 300 single-shot measurements and are compared with the those obtained from the nephelometry measurements. The $\bar{C}(r,z)$ for both techniques are compared at 3.0 and 4.5 nozzle diameters downstream from the exit plane, as shown in Figures 6(a) and 6(b). The $\bar{C}(r,z)$ is calculated via the following equation, whereby $C_i(r,z)$ is the i^{th} single-shot measurement and N is the number of images recorded [28, 29]:

$$\bar{C}(r,z) = \frac{1}{N}\sum_{i=1}^{N} C_i(r,z) \ . \tag{1}$$

From Figure 6(a), it is apparent that the average profiles of the measurements are quite uniform through the jet. Such distribution is to be expected for the potential core region and has been widely observed by others in similar flow fields. This observation suggests that, on average, both the indium-LIF and the scattered light signal from the particulates are representative of the concentration profile of the jet issuing from the nozzle. From Figure 6(b), it is also clear that the profiles of the measurements exhibit a central region where the concentration is still uniform at 4.5 nozzle diameters above the exit plane, caused by the tip of the potential core at this height. This finding is consistent with the results of previous studies (*e.g.*, [30]), in which the potential core of jet issuing from a pipe is generally expected to last five nozzle diameters downstream from the exit plane. Furthermore, this length is greater for a laminar flow, and with a co-flow, than for a free jet.

From Figures 6(a) and 6(b), it is apparent that there are small but sig-

(a)

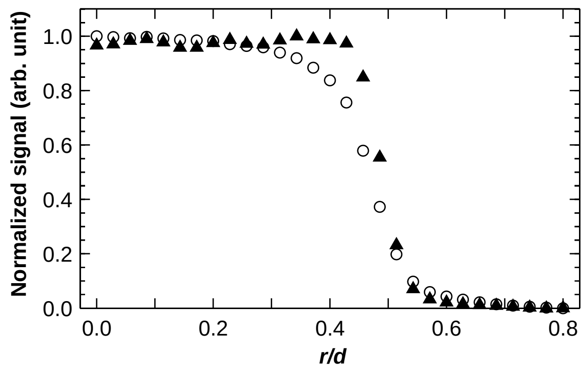

(b)

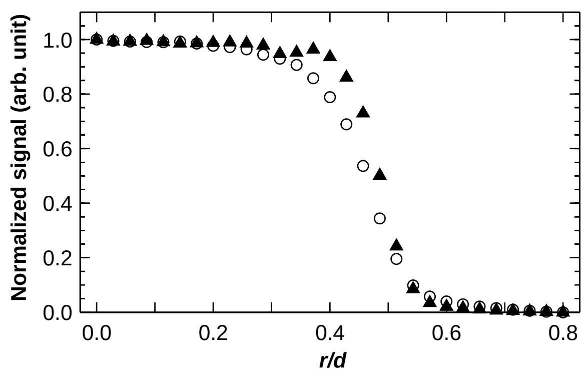

Figure 6: The average radial profiles $\bar{C}(r, z)$ as obtained from 300 instantaneous measurements at *z/d:* (a) 3.0 and (b) 4.5 nozzle diameters above the exit plane. Open circles: indium-LIF. Closed triangles: nephelometry signal.

nificant differences between the LIF and the nephelometry profiles. That is the indium-LIF signal decreases with radial distance at a slightly greater rate that the nephelometry signal. The slight disparity of the profiles may be explained by the possible departure of the trajectories of the particles from those of the molecular field or the effects of molecular quenching on the indium-LIF signal.

The extent to which the ablation-generated particles fail to act as flow-tracers has been evaluated on the basis of their Stokes number (Sk):

$$Sk = \rho_p U d_p^2 / 18 \mu L \ , \tag{2}$$

which characterises the particle response time to the fluid flow time associated with an eddy of scale L. Here, ρ_p corresponds to the particle density, which is taken to be the 7200 kg/m^3 on the basis of an assumed composition of indium oxide [31], μ is the absolute viscosity and L is assumed to be the nozzle diameter d. Calculations reveal that to act as a flow tracer, *viz.* Sk<<1, it is necessary for the particle diameters d_p to be of order ∼1.6 µm. While the size distribution of the ablation-generated products is not known, there is indication that the nephelometry signal (as evident from the instantaneous nephelometry images) is dominated by particles of size greater than this and with, at best, a partial response to the flow. Further evidence can also be found by comparing the width of the measured potential core region by the two techniques in Figures 6(a) and 6(b). The width of the potential core region extends to r/d≈0.45 and 0.40 for the nephelometry signal, and

0.30 and 0.20 for the indium-LIF signal, at z/d=3.0 and 4.5. The width measured by the nephelometry technique is much larger than expected for a potential core. Together, these findings indicate that size of the ablation-generated particles is more likely to be the main cause for the discrepancy between the nephelometry and the LIF signals, than the effects of molecular quenching.

It is also important to note that while nephelometry is a well established technique for concentration measurements [28, 29, 32], the signal can only be assumed to be directly proportional to the total number of particles in the measurement region if the particle size distribution is constant. Nevertheless, any variations in particle size are likely to be smoothed out in the mean image. The $\bar{C}(r,z)$ for the nephelometry measurements is non-dimensionalised by dividing the $\bar{C}(r,z)$ with the summation of the $\bar{C}(r,z)$ at each measurement locations.

To further assess the feasibility of the techniques to map the concentration profile of the jet, the RMS of the measurements, $\tilde{C}(r,z)$, is calculated as:

$$\tilde{C}(r,z) = \frac{1}{N}\left(\sum_{i=1}^{N}\left(C_i(r,z) - \bar{C}(r,z)\right)^2\right)^{\frac{1}{2}} , \tag{3}$$

The results for the $\tilde{C}(r,z)/\overline{C}(r,z)$ for the nephelometry and indium-LIF measurements, recorded at 3.0 and 4.5 nozzle diameters downstream from the exit plane, are shown in Figures 7(a) and 7(b). From Figure 7(a), it is clear that the RMS of the two techniques are typically lower than 2%

(a)

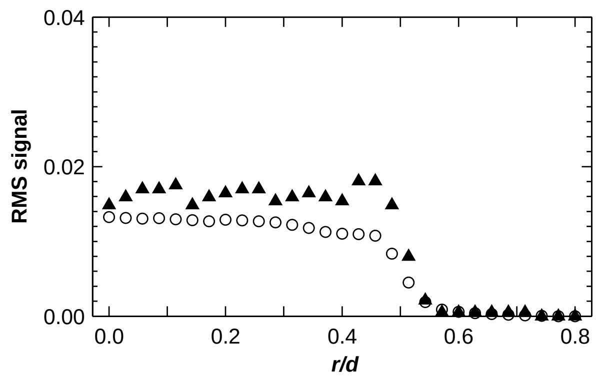

(b)

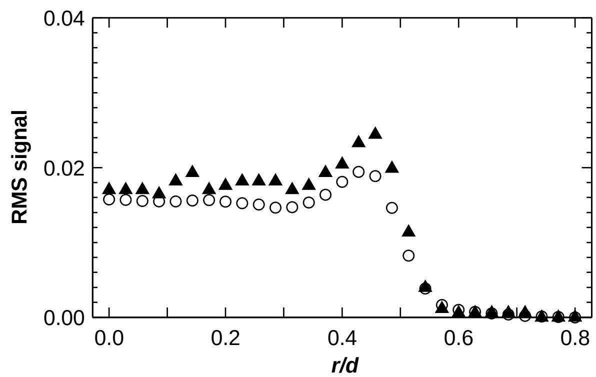

Figure 7: The RMS of the radial profiles $\bar{C}(r, z)$ as obtained from 300 instantaneous measurements at *z/d:* (a) 3.0 and (b) 4.5 nozzle diameters above the exit plane. Open circles: indium-LIF. Closed triangles: nephelometry signal.

and are observed to display a region of uniformity across the jet, which is to be expected when measuring a laminar jet. The RMS of the techniques, albeit low, is mainly associated with the fluctuation in the amount of seeded species within the measurement region. It is worth noting that the RMS of the nephelometry signal is found to be 33% higher than the indium-LIF signal. This is a result of the inherently polydispersed nature of the ablation products size. The use of such non-uniform ablation products would increase the RMS of the nephelometry measurements, since the larger particles scatter the radiation more efficiently that the smaller ones [28]. From Figure 7(b), it is found that the RMS of the indium-LIF and the nephelometry signals increases in the shear layer. Nonetheless, it is noted that the distribution of the RMS for both techniques is still below 2% at the potential core of the jet. Again, the RMS of the nephelometry signal is found to be $\sim$15% higher than the indium-LIF.

5 Conclusion

This paper presented the first demonstration of pulsed laser ablation technique to seed a laminar non-reacting gaseous jet at atmospheric pressure. The neutral indium atoms generated have been found to be stable and survive a convection time of tens of seconds before entering the interrogation region. A comparison of the laser-induced fluorescence (LIF) of the indium with the nephelometry measurements of the ablation products, both generated by the pulsed laser ablation technique, revealed good agreement, given the high Stokes number of the ablation products. That is, the slightly wider spread of the ablation particles over the indium gas is consistent with the nephelometry signal being influenced by particles with, at best, a partial response to the flow. Likewise, the higher root mean square (RMS) of the ablation products is consistent with the particulate nature of the nephelometry marker. Future work, however, is required to evaluate the effects of molecular quenching. This paper has also shown that the spurious scattered signal from the particulates larger than $\sim$1 μm can be effectively suppressed from the indium LIF signal, thus confirming the suitability of the method for use in other particle-laden environments, such as in the presence of particle seeding for particle image velocimetry (PIV). These results demonstrated the feasibility of using pulsed laser ablation to provide scalar markers for mixing studies. Nevertheless, further work is required to quantify the performance of indium as a scalar marker.

Acknowledgments

The authors wish to acknowledge the support of the Centre for Energy Technology (CET) and The University of Adelaide. The Australian Research Council (ARC) is also gratefully acknowledged for their funding support of this work through ARC Discovery and Linkage Infrastructure, Equipment and Facilities (LIEF) grant schemes. The authors are thankful to A/Prof.

Greg Metha from the School of Chemistry and Physics, Mr Eric Hsu from the School of Chemical Engineering, and Mr Saleh Mahmoud from the School of Mechanical Engineering for their assistance with this project.

References

[1] R. E. Rosensweigh, H. C. Hottel, and G. C. Williams, "Smoke-scattered light measurement of turbulent concentration fluctuations," Chemical Engineering Science **15**, 111–129 (1961).

[2] N. H. Qamar, Z. T. Alwahabi, Q. N. Chan, G. J. Nathan, D. Roekaerts, and K. D. King, "Soot volume fraction in a piloted turbulent jet non-premixed flame of natural gas," Combustion and Flame **156**, 1339–1347 (2009).

[3] N. H. Qamar, G. J. Nathan, Z. T. Alwahabi, and Q. N. Chan, "Soot sheet dimensions in turbulent nonpremixed flames," Combustion and Flame p. doi: 10.1016/j.combustflame.2011.04.017 (2011).

[4] G. J. Nathan, J. Mi, Z. T. Alwahabi, G. J. R. Newbold, and D. S. Nobes, "Impacts of a jet's exit flow pattern on mixing and combustion performance," Progress in Energy and Combustion Science **32**, 496–538 (2006).

[5] P. R. Medwell, P. A. M. Kalt, and B. B. Dally, "Simultaneous imaging of OH, formaldehyde, and temperature of turbulent nonpremixed jet

flames in a heated and diluted coflow," Combustion and Flame **148**, 48–61 (2007).

[6] P. R. Medwell, P. A. M. Kalt, and B. B. Dally, "Imaging of diluted turbulent ethylene flames stabilized on a jet in hot coflow (JHC) burner," Combustion and Flame **152**, 100–113 (2008).

[7] A. Y. Klimenko, "Multicomponent diffusion of various admixtures in turbulent flow," Fluid Dynamics **25**, 327–334 (1990).

[8] N. Peters, "Laminar flamelet concepts in turbulent combustion," Proceedings of the Combustion Institute **21**, 1231–1250 (1988).

[9] R. S. Barlow, "Laser diagnostics and their interplay with computations to understand turbulent combustion," Proceedings of the Combustion Institute **31**, 49–75 (2007).

[10] J. H. Frank, K. M. Lyons, D. F. Marran, and M. B. Long, "Mixture fraction imaging in turbulent nonpremixed hydrocarbon flames," Proceedings of the Combustion Institute **25**, 1159–1166 (1994).

[11] G. J. Nathan, P. A. M. Kalt, Z. Alwahabi, B. B. Dally, P. R. Medwell, and Q. N. Chan, "Recent advances in the measurement of strongly radiating, turbulent reacting flows," Progress in Energy and Combustion Science p. doi: 10.1016/j.pecs.2011.04.001 (2011).

[12] A. G. Hsu, V. Narayanaswamy, N. T. Clemens, and J. H. Frank, "Mixture fraction imaging in turbulent non-premixed flames with two-photon LIF of krypton," Proceedings of the Combustion Institue **33**, 759–766 (2011).

[13] M. Eyett and D. Bäuerle, "Influence of the beam spot size on ablation rates in pulsed-laser processing," Applied Physics Letters **51**, 2054–2055 (1987).

[14] S. Preuss, E. Matthias, and M. Stuke, "Sub-picosecond UV-laser ablation of Ni films: Strong fluence reduction and thickness-independent removal," Applied Physics A **59**, 79–82 (1994).

[15] S. Preuss, A. Demchuk, and M. Stuke, "Sub-picosecond UV laser ablation of metals," Applied Physics A **61**, 33–37 (1995).

[16] J. Bakos, I. Földes, P. N. Ignácz, G. Kocsis, J. Szigeti, and J. Kovács, "Absolute measurement of velocity distribution of neutrals in sodium laser blow-off beam," Optics Communications **74**, 374–379 (1990).

[17] C. Breton, C. de Michelis, W. Hecq, and M. Mattioli, "Low energy neutral beam production by laser vaporization of metals," Revue De Physique Appliquee **15**, 1193–1200 (1980).

[18] K. Alti and A. Khare, "Low-energy low-divergence pulsed indium atomic beam by laser ablation," Laser and Particle Beams **24**, 47–53 (2006).

[19] J. E. Sansonetti and W. C. Martin, "Handbook of basic atomic spectroscopic data," Journal of Physical and Chemical Reference Data **34**, 1559–2259 (2005).

[20] I. S. Burns, J. Hult, G. Hartung, and C. F. Kaminski, "A thermometry technique based on atomic lineshapes using diode laser LIF in flames," Proceedings of the Combustion Institute **31**, 775–782 (2007).

[21] I. S. Burns, X. Mercier, M. Wartel, R. S. M. Chrystie, J. Hult, and C. F. Kaminski, "A method for performing high accuracy temperature measurements in low-pressure sooting flames using two-line atomic fluorescence," Proceedings of the Combustion Institute **33**, 799–806 (2011).

[22] P. R. Medwell, Q. N. Chan, P. A. M. Kalt, Z. T. Alwahabi, B. B. Dally, and G. J. Nathan, "Development of temperature imaging using two-line atomic fluorescence," Applied Optics **48**, 1237–1248 (2009).

[23] J. E. Dec and J. O. Keller, "High speed thermometry using two-line atomic fluorescence," Proceedings of the Combustion Institute **21**, 1737–1745 (1986).

[24] Q. N. Chan, P. R. Medwell, P. A. M. Kalt, Z. T. Alwahabi, B. B. Dally, and G. J. Nathan, "Simultaneous imaging of temperature and soot volume fraction," Proceedings of the Combustion Institute **33**, 791–798 (2011).

[25] Q. N. Chan, P. R. Medwell, Z. T. Alwahabi, B. B. Dally, and G. J. Nathan, "Assessment of interferences to nonlinear two-line atomic fluorescence (NTLAF) in sooty flames," Applied Physics B **104**, 189–198 (2011).

[26] Q. N. Chan, P. R. Medwell, P. A. M. Kalt, Z. T. Alwahabi, B. B. Dally, and G. J. Nathan, "Solvent effects on two-line atomic fluorescence of indium," Applied Optics **49**, 1257–1266 (2010).

[27] C. F. Kaminski, J. Engström, and M. Aldén, "Quasi-instantaneous two-dimensional temperature measurements in a spark ignition engine using 2-line atomic fluorescence," Proceedings of the Combustion Institute **27**, 85–93 (1998).

[28] M. B. Long, B. T. Chu, and R. K. Chang, "Instantaneous two-dimensional gas concentration measurements by light scattering," AIAA Journal **19**, 1151–1157 (1981).

[29] M. B. Long, B. F. Webber, and R. K. Chang, "Instantaneous two-dimensional concentration measurements in a jet flow by Mie scattering," Applied Physics Letter **34**, 22–24 (1979).

[30] J. Mi, D. S. Nobes, and G. J. Nathan, "Influence of jet exit conditions on the passive scalar field of an axisymmetric free jet," Journal of Fluid Mechanics **432**, 91–125 (2001).

[31] Available from: <http://msds.chem.ox.ac.uk/> .

[32] H. A. Becker, H. C. Hottel, and G. C. Williams, “On the light-scatter technique for the study of turbulence and mixing,” Journal of Fluid Mechanics **30**, 259–284 (1967).